International Journal of Engineering & Technology, 7 (4.18) (2018) 442-448

International Journal of Engineering & Technology

Website: www.sciencepubco.com/index.php/IJET

Research paper

Implementation of Two Stage Isolated Multilevel Inverter Control Strategy Using Fuzzy Logic Controller for Photovoltaic Application

[1]K. Jithendra Gowd, [2]K. Pavani, [3]K. Nagabhushanam

JNTUA College of Engineering, Ananthapuramu, A.P, India
**Corresponding author E-mail: indra.jithu@gmail.com,*

Abstract

The Photovoltaic (PV) is an unavoidable segment in renewable energy based power generation system. The two stage power conversion is a best pay tribute to grid-connected PV systems. Nevertheless, the power converters design and control integration must be prized to achieve the efficiency and reliability. In this paper, the implementation of control strategy for dual stage inverter is presented using fuzzy logic controller (FLC) along the higher frequency isolation which is galvanized. Dual stage converter contains the DC-DC converter which is three phase series resonance converter which functions as switch frequency of converter is equal to the resonance frequency. The DC-DC converter mainly provides a bus along with voltage balancing on multilevel converter. Another stage of dual stage inverter is DC-AC arrangement that comprises of a NPC (Neutral Point Clamped) inverter which is intended to inject current into the grid. The operating stages of inverter provide the internal transfer function, and also the external transfer function was obtained by considering the reverse energy flow. Dual-stage inverter with FLC is simulated and tested, resulting in lower Total Harmonic Distortion (THD).

Keywords: *Neutral Point Clamping inverter; Two-stage multilevel inverter; Fuzzy Logic Controller; Membership functions; Total harmonic distortion.*

1. Introduction

Recently, varied photovoltaic (PV) systems are developing for generation of energy which is renewable. PV systems which are of miniature scale about 15KW are rising within the marketplace of building integrated electrical PV systems [1], [2]. The above systems generally need a three-phase inverter which has isolation to convert direct voltage obtained from PV panels into alternating voltage and then inject it into the grid. The electrical converter with galvanic measurability, however they will give solution used for security issues and gives voltage and current quite significant and really pricy .Worldwide growth of PV's is very dynamic and varies powerfully by country [2]. By the tip of 2016, accumulative PV capacity accrued by over seventy five Giga Watt (GW) and reached a minimum of 303 GW, comfortable to produce 1.8% of the inward and other transfer capacities. The highest installers in 2016 were China, the U.S., and India. There square measure over twenty four countries round the world with accumulative PV capability of over one GW. Australia, Chile, and South Africa, all crossed the one GW-mark in 2016.

The obtainable PV capability in Central American country is currently comfortable to produce 12.5% of the nation's power whereas European country, Federal Republic of Germany and Hellenic Republic will turn out between seven members and eight of their various domestic electricity consumption [3], [5]. According to this information, it is conceivable to examine the significance along the propensity to research fresh wellspring of elective power. The age of power from sun homeward-bound PV modules was considered in this paper. At the purpose once PV modules are interconnected with the utility grid, the energy supply to the loads may increase; however for infusing the modified energy from the PV modules it is vital to utilize static power converters. Some converter technologies are presented; they may be one or else two stages, and also controlling methodologies with FLC are used for functioning of the PV system.

During this approach, this paper displays the execution of a two-arrange electrical converter, together with a three-level NPC electrical in its structure converter. A structure electrical converter topology offers a response to scale back voltage stress at every component from incrementing the quantity of levels [3]. Moreover, by using highly developed modulation methods for the PV system mitigation of the leak current may achieve.
Section 2 provides the two stage converter and its topology. The DC-DC converter and its utilization is talked about in Section3. The NPC inverter operating stages and its important expressions are discussed in section 4. Modeling techniques of internal and external control loops are explained in section 5. Section 6, provides the results obtained from simulation of structure. The conclusion of whole system is given in section 7.

2. Two-stage converter topology

The structure of two stage electrical converter topology is presenting in this paper. Also it develops preceding systems as well as progresses the presentation of converter. Dual stage converter has a structure as shown in Fig.1. Within the planned topology, one

variety of NPC multilevel inverter as well as DC-DC converter are incorporated to cut back the switches and direct current sources which are of large amount. The primary arrangement is created out of a DC-DC resonating converter along with a transformer, each three-stage and dealing at high frequency, during this manner decreasing the dimensions and weight of the electrical device. Two Graetz spans are associated with the optional transformer windings, also the NPC inverter along with a capacitive bus associated with these windings. The NPC inverter is intended as a next stage in structure to discharge current into the electric grid [1].

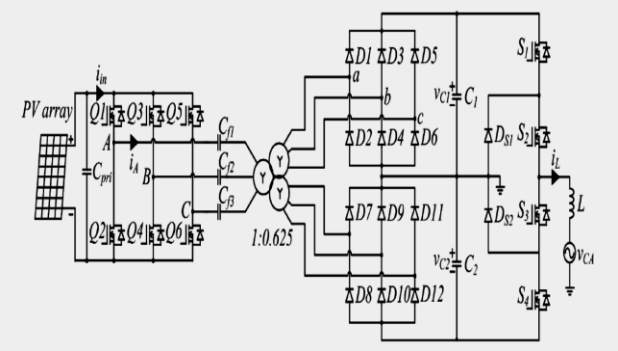

Fig. 1: Structure of the two-stage converter

3. DC-DC converter

In this paper, isolated DC-DC power converter and NPC multi-level inverter (MLI) are designed for a standalone PV system which is most suitable to both domestic and industrial applications and converter reduces the voltage balancing problem in MLI while converting DC to AC. Fig. 2 presents the structure of DC-DC power converter, here the inductances of line discipline as the transformer inductances also, R loss is the loss circulated by the course. This DC-DC converter arrangement provides higher switch frequency and higher efficiency along with soft switching capability [6], [7].

3.1 Efficiency calculation

The capacitance and inductance of DC-DC converter are identical in order to verify that diodes of graetz bridges provide concurrent switching relating to the transistors of converter. In this case the voltage across the converter points A, B, and C is maintained in phase with respect to the voltage across a, b, and c points which depicted in fig.2. So that, the voltage across the filter circuit may obtain from the difference of the above voltages. This strategy was followed in order to get (1).

$$i_A = \frac{2}{\pi}\frac{1}{\mathrm{R_{loss}}}(V_{in} - V'_1)sen(\omega t) \quad (1)$$

Here, R_{loss} is said to be the parasitic protections circulated through the circuitry; V_{in} is the voltage input to the converter; V'1 is the reflected voltage at output; i_A is converter line current. The input current (i_{in}) is equivalent to the phase current (i_A) about the scope of 60 ° to 120°. The DC-DC converter contains the synchronism between focuses A and a so that the output current is concluded as reflected phase current. The mean estimation of the above current might be gotten by (2).

$$I_{inmed} = \frac{6}{\pi^2}\frac{1}{\mathrm{R_{loss}}}(V_{in} - V'_1) \quad (2)$$

Hence, the DC-DC converter had contained input power as (3) and provided output power as (4) which are figured as

$$P_{in} = V_{in} I_{inmed} \quad (3)$$

$$P_1 = V'_1 I_{inmed} \quad (4)$$

The efficiency of DC-DC converter is estimated using (3), (4) it might be provided in (5)

$$\eta = \frac{V'_{out}}{V_{in}} \quad (5)$$

The DC-DC converter provides a higher efficiency of around 97%, which might be estimated to a unit position. In this manner, as (5) could provide an immediate connection between the output and the input voltages.

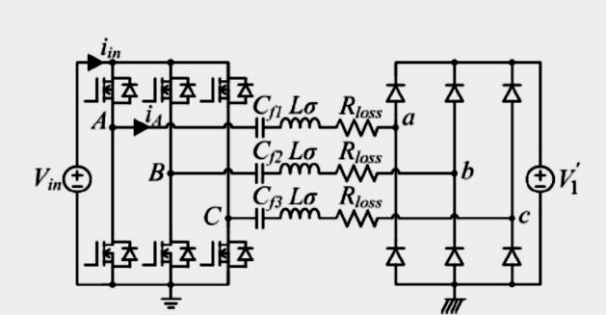

Fig. 2: Transformer less DC-DC converter

4. Operation stages and primitive inverter equations

NPC inverter under goes a modulation technique in which the triangular carrier wave contains identical frequency and magnitude, although they are dispersed in the form that there is distinct band gap between the carrier waves [1], [2].

4.1 NPC operation stages

The dead time in the commencement of switches of NPC inverter was not found here due to the consideration of an ultimate inverter in the present paper. By the utilization of modulation there are four stages presented here for NPC inverter operation, as depicted in Fig.3.

In first stage of operation, switches S_1 and S_2 are turned on when the switches S_3 and S_4 are turned off. So that, the flow of current takes place through the capacitor C_1 to V_{CA} which is the load, resulting the positive voltage in the lattice.

For the second stage, switches S_1 and S_4 turned on while S_2 and S_3 switches are turned off. Because of positive peak of modulating wave which is sinusoidal, there is a flow of energy to load only through the clipping diode D_{s_1} resulting a freewheeling mode for inverter. There is no flow of current through C_1 leading zero level of voltage.

The previous steps are continued until reaching the negative peak of modulation wave. During the third stage S_1 and S_2 are turned off when the switches S_3 and S_4 are turned on for providing the current flow through the capacitor C_2 to the load which results in the negative voltage on lattice.

As following the above process in the fourth stage, switches S_1 and S_4 turned off while S_2 and S_3 switches are turned on. Because of negative peak of modulating wave which is sinusoidal, there is a flow of energy to load only through the clipping diode D_{s_2} providing a freewheeling mode for inverter. There is no flow of current through C_2 leading zero level of voltage.

The final steps are continued until reaching the positive peak of modulation wave. The modulation wave of inverter and the volt-

ages occurred in the operating stages along the switching are depicted in the Fig.4.

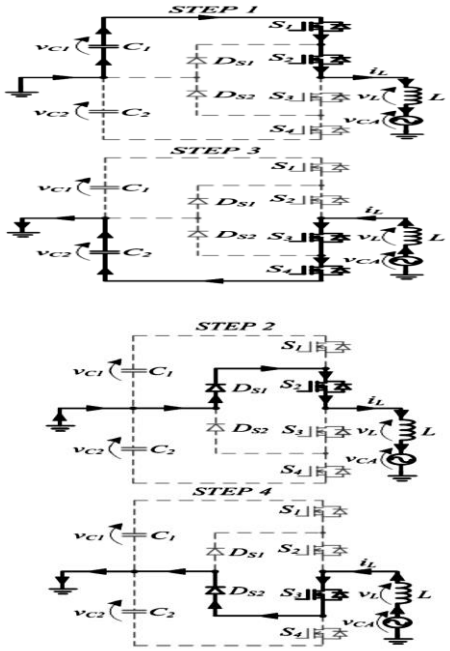

Fig.3: Inverter operation stages

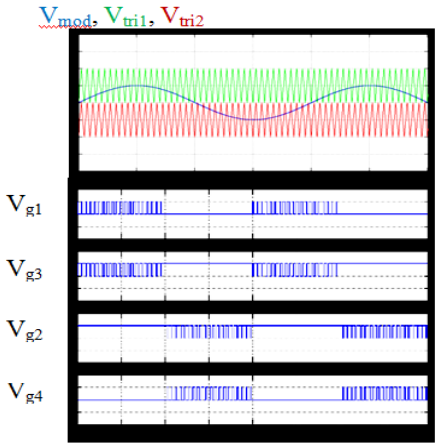

Fig. 4: Waveforms of NPC inverter

4.2. Main inverter calculations

The first two phases of task were utilized in the estimation of values of the fundamental parts of NPC inverter as the further two steps are integral. The expressions for this section were obtained by utilizing Fig. 5

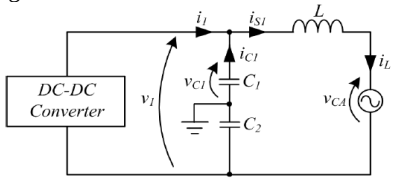

Fig. 5: Equivalent circuit for first stage of operation of NPC inverter

4.2.1. Static voltage gain

The equivalent circuit of the first two steps of NPC operation under goes mesh analysis for obtaining the current differentiation which related with the inductor. The mean square of this derivative might provide (6). V_1 is the addition of voltages of V_{C1} and V_{C2}.

$$\frac{di_L}{dt} = \frac{V_1}{2L}D - \frac{V_{CA}}{L} \tag{6}$$

Here: V_1 is the NPC bus voltage; V_{CA} is the voltage across grid; D is the obligation cycle; L is the inductance of output filter; $\frac{di_L}{dt}$ is the immediate subordinate of inductor current. When the differentiation of current is zero for stable inverter, then (6) prompts (7), which represents the characteristics of inverter output considering the duty cycle. So that it was observed that V_1 might be more than the V_{CA} even when the duty cycle was unique.

$$\frac{V_{CA}}{V_1} = \frac{D}{2} \tag{7}$$

4.2.2. Estimation of the output inductance

The current infusing through the grid might be a sine wave form because of output inductance. Considering (7) and also the sine envelope of duty cycle there produced (8).

$$D(\omega_{grid}t) = \frac{2}{V_1}V_{CA_P}\text{sen}(\omega_{grid}t) \tag{8}$$

Here: $V_{CA_P}$is the max voltage of the grid; ω is the angular frequency of the grid. First stage of operation of NPC inverter under goes loop analysis for providing (9).

$$\Delta i_L = \frac{V_1 D}{2f_s L} - \frac{V_{CA}D}{f_s L} \tag{9}$$

Where: $f_s$is the exchanging frequency; $\Delta i_L$is the swell in the inductor. On Substituting (8) in (9) which provides (10).

$$\Delta i_L = \frac{V_{CA_P}\text{sen}(\omega_{grid}t)}{f_s L} - \frac{2(V_{CA_P})^2\text{sen}^2(\omega_{grid}t)}{V_1 f_s L} \tag{10}$$

When the inductor contains larger ripple in the current then it is said to be it was designed in such a worst case. Subsequently, the utilization of most extreme point takes place; in that case the differentiation of current is zero. At that point (10) prompts (11).

$$\text{sen}(\omega_{grid}t) = \frac{V_1}{4V_{CA_P}} \tag{11}$$

The largest ripple in the inductor current was expressed in (11), again substituting this in (10) provides (12) which represents the inductor equation of NPC inverter circuit.

$$L = \frac{V_1}{8f_s \Delta I_{Lmax}} \tag{12}$$

4.2.3 Scaling of bus capacitors in NPC inverter

For analysis purpose only one capacitor was considered in the scaling process. However, the procedure is esteemed for both capacitors in the NPC inverter circuit. Fig. 5 provided the instant power input across the inverter it might be composed as (13).

$$P_1(t) = V_{CA_P} I_{L_P} \text{sen}^2(\omega_{grid}t) \tag{13}$$

Here: P_1 is the NPC inverter power input; I_{L_P}peak current input of the NPC inverter. Utilizing trigonometric formulations there is a realization for voltage V_{CA} that it has no precise relocation and it is a sine wave, Therefore (14) is acquired.

$$P_{out}(t) = P_{outmed} - P_{outmed}\cos(2\omega_{rede}t) \tag{14}$$

The instant power output of NPC inverter was provided in (14) which consisted of two sections that are steady power output and

variable power output. The currents i_{s1}, i_{C1}, and i_1 are analyzed in order to estimate i_{s1} as mean value of addition of i_{C1} and i_1. This characteristic can provide the estimation of (15).

$$V_{C1} i_{C1} = P_{med} \cos(2\omega_{grid} t) \quad (15)$$

Utilizing the expression of capacitor voltage as well as taking into account the most extreme ripple in voltage of the capacitor, (16) is gotten.

$$C_1 = \frac{P_{med}}{\omega_{grid}\, V_{C1}\, \Delta V_{C1max}} \quad (16)$$

Here: ΔV_{C1max} is the most extreme swell in the voltage of capacitor of NPC inverter.

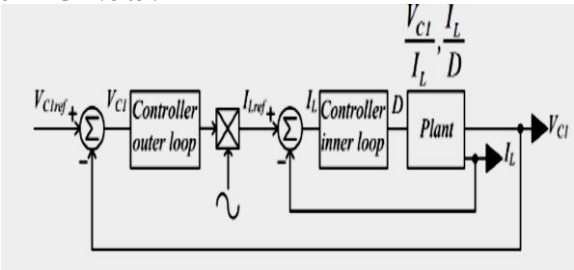

Fig. 6: Inverter control loops block diagram

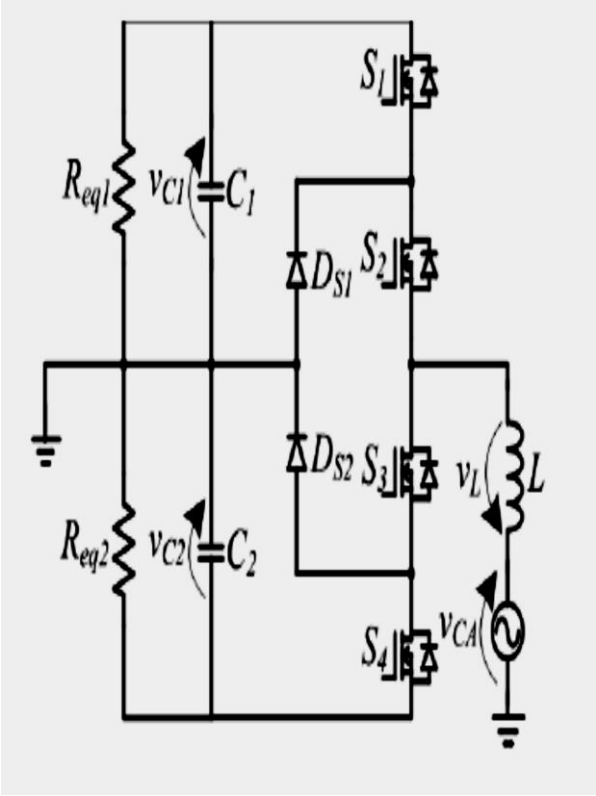

Fig. 7: NPC as rectifier.

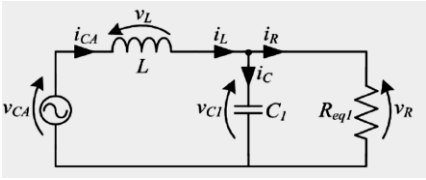

Fig. 8: Equivalent circuit for NPC first stage operation as rectifier.

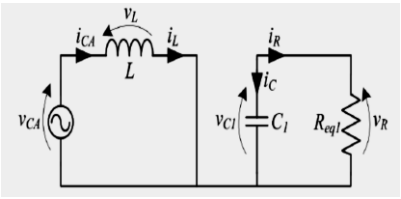

Fig. 9: Equivalent circuit for the NPC second stage of operation as rectifier

5. Modeling and determination of the inverter transfer functions

The control mechanism of two stage inverter was modeled as two control loops which provide inner transfer function (current control loop) as well as outer transfer function(voltage control loop). The control mechanism is depicted by means of block diagram in Fig.6 [1].

5.1. Internal transfer function

This transfer function was obtained from sufficient application of Linearization technique using Jaccobian in (6), after that Laplace transform would provide to obtain (17).

$$G_1 = \frac{I_L(s)}{D(s)} = \frac{V_1}{2Ls} \quad (17)$$

Where: I_L is the current in the inductor.

5.2. External transfer function

For obtaining this tansfer function, NPC inverter was considered as a rectifier and its equivalent circuit is also provided in Fig.7. According to four stages of NPC operation preceding two stages might provide the rectifier circuit which reponsible for reverse energy flow. These circuits are equivalent to the outer loop control of NPC Which are depicted in Fig. 8 and Fig. 9.These circuits are applicable in the mesh and nodal analysis respectively for obtaining (18), (19).
The differentiation of current and voltage of the circuits which reffering inductor and capacitor are mean squared to obtain (18)and(19). These are represented as non linearized state expressions.

$$\frac{di_L}{dt} = \frac{V_{CA}}{L} - \frac{V_1}{2L} D \quad (18)$$

$$\frac{dV_{C1}}{dt} = \frac{i_L}{C_1} D - \frac{V_{C1}}{R_{eq1} C_1} \quad (19)$$

Here: R_{eq1} is the equivalent resistant.

By using the Jaccobian technique, (18) and (19) are Linearized about an operating point. The equations of linearization were represented in the form of state space bringing about (20) and (21).

$$\begin{bmatrix} \frac{di_L}{dt} \\ \frac{dV_{C1}}{dt} \end{bmatrix} = \begin{bmatrix} 0 & -\frac{\vec{D}}{L} \\ \frac{\vec{D}}{C_1} & -\frac{1}{R_{eq1}} \end{bmatrix} \begin{bmatrix} I_L \\ V_{C1} \end{bmatrix} + \begin{bmatrix} -\frac{\overrightarrow{V_{C1}}}{L} \\ \frac{\vec{i_L}}{C1} \end{bmatrix} [D] \quad (20)$$

$$y = [0 \quad 1] \begin{bmatrix} I_L \\ V_{C1} \end{bmatrix} \quad (21)$$

The bars on a few factors might represent which are consistent and also which are in stable state. From Beginning (20) and (21) are responsible for the external transfer function so that provided the voltage over the capacitor C1 along the duty cycle for attaining (22).

$$G_2(s) = \frac{V_{C1}(s)}{D(s)} = -\frac{\left[\frac{\overrightarrow{V_{C1}}}{\vec{D}}\right]\left[1 - s\frac{L\overrightarrow{I_L}}{\overrightarrow{V_{C1}}\vec{D}}\right]}{1 + s\frac{L}{\overrightarrow{D^2}R_{eq1}} + s^2\frac{LC_1}{\overrightarrow{D^2}}} \quad (22)$$

The current with respect to the inductor along the duty cycle which is related in the formation of transfer function is in (23), it might be enough for inverse result of (21)

$$y = [0 \quad 1]\begin{bmatrix} I_L \\ V_{C1} \end{bmatrix} \quad (23)$$

This similar strategy was followed which bring about (22) and (23), (24) is gotten.

$$G_3(s) = \frac{I_L(s)}{D(s)} = -\frac{R_{eq1}LC_1\left[s\frac{\overrightarrow{V_{C1}}}{L} + \frac{\overrightarrow{V_{C1}}}{R_{eq1}LC_1} + \frac{\vec{D}\overrightarrow{I_L}}{LC_1}\right]}{\overrightarrow{D^2}R_{eq1} + sL + s^2R_{eq1}LC_1} \quad (24)$$

To acquire the external transfer function, it is sufficient to isolate (22) by (24), obtaining (25).

$$G_4(s) = \frac{V_{C1}(s)}{I_L(s)} = \frac{\overrightarrow{V_{C1}}\vec{D} - sL\overrightarrow{I_L}}{sC_1\overrightarrow{V_{C1}} + \frac{\overrightarrow{V_{C1}}}{R_{eq1}} + \vec{D}\overrightarrow{I_L}} \quad (25)$$

From (17) and (25), the transfer functions of inner and outer control loops of the inverter control mechanism are specified.

5.3 Fuzzy logic controller (FLC):

Fuzzy logic may be a sort of many-valued logic; in this logic the reality value of variable is whichever numeric value from zero to one. Against this, Boolean logic provides the reality value of variable might solely either zero or one. FLC had to provide the conception of truth which is a biased value, wherever the reality value might vary between fully true and fully false.

Generally, FLC system contains four most important elements: fuzzification stage, fuzzy inference engine, and fuzzy rule base and defuzzification stage. Fig.10 provides the schematic procedure for FLC operation. There are 3 major steps for the general application of fuzzy logic to any system.

1. Fuzzification– which converts classical information or crisp information into fuzzy information.

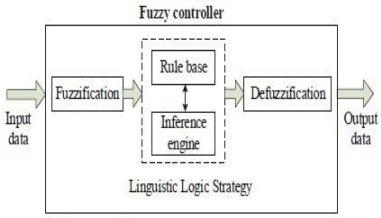

Fig.10: Fuzzy logic controller

2. Fuzzy inference method – MFs are combined to the rules of FLC for deriving the controller output.

3. Defuzzification – various strategies are utilized for computing respective outputs which are placed in a table that called as the look up table. The outputs are developed using this look up table which supported the respective input throughout associate degree of application. Fig.11and 15 showing the simulation of FLC control loop, and FLC simulation block.

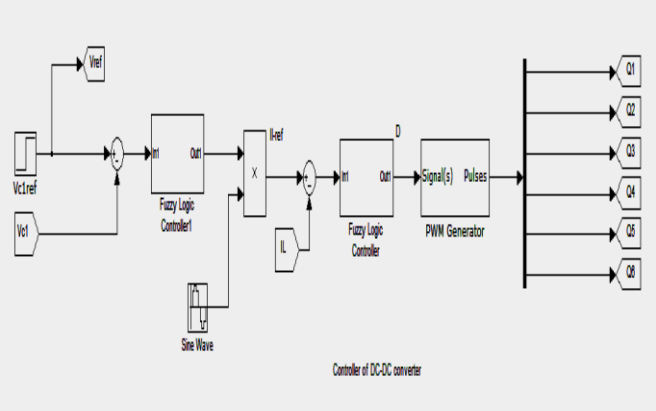

Fig.11: Simulation block of FLC control loop

5.3.1. Fuzzification:

fuzzification involves 2 processes: derivation of input as well as output MFs and pointing of linguistic variables to the MFs. There are different shapes of MFs, like Triangular wave shape, tetragon wave shape, Gaussian wave shape, convex wave shape, sigmoid wave shape and S-curve wave shape. The values of MFs are appointed to the linguistic variables, to attain 7 fuzzy sub groups: NH (Negative High), NM (Negative Medium), NS (Negative Small), ZE (Zero), PS (Positive Small), PM (Positive Medium), and PH (Positive High). The Fuzzy sub sets are grouped in the form of MFs for providing error and change in error of input parameters in order to get steady values of system. As shown in below Fig.12, 13, and 14 the input and output membership functions are provided.

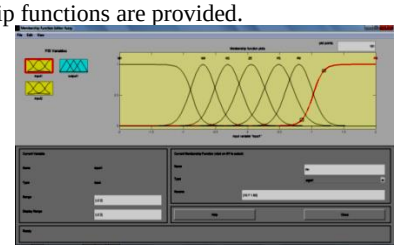

Fig. 12: Input1 as error in load current, E (k) membership functions

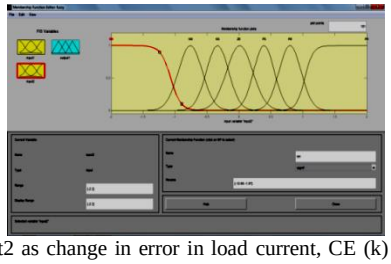

Fig.13: Input2 as change in error in load current, CE (k) membership functions

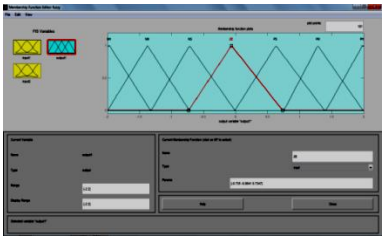

Fig.14: Output MFs

5.3.2. Inference Method:

Many composite strategies like Max-Min and Max-Dot are planned within literature. Min technique was employed for this strategy. In every rule the output MF might represent with the

max as well as min operator. Table 1 shows the rule base of the FLC.

5.3.3. Rule Base:

In a rule the 'If' aspect was named as the antecedent, the 'Then' aspect was named as the consequence which resemble thoughts of a person. In a rule base linguistic variables are assessed for fuzzification to execute the principles.

Table.1: Rule Matrix

Error	Change in Error						
	Nh	Nm	Ns	Ze	Ph	Pm	Ps
Nh	Nh	Nh	Nh	Nh	Nm	Ns	Ze
Nm	Nh	Nh	Nh	Nm	Ns	Ze	Ns
Ns	Nh	Nh	Nm	Ns	Ze	Ns	Nm
Ze	Nh	Nm	Ns	Ze	Ze	Pm	Ph
Ph	Pm	Ps	Ze	Ps	Pm	Ph	Ph
Pm	Pm	Ze	Ps	Pm	Ph	Ph	Ph
Ps	Ze	Ps	Pm	Ph	Ph	Ph	Ph

5.3.4. Defuzzification:

Mamdani model was favored in this situation since this was succeeded to the Compositional Rule provided through inference in its fuzzy interpretation method. For estimating the FLC outage, 'centroid' technique was utilized so that the control loop output was modified by means of output of FLC. Then, the switching of the inverter might control through the FLC outage. In two stage inverter structure, NPC Inverter is in charge of the bus voltage control as well as the controlling of grid current**.** This controlling process was achieved by considering as well as contrasting the reference value with noted variables. For achieving this control strategy, the MFs of FLC are: error, change in error and output.
The FLC rules are deposited by using below expression

$$u=-[\alpha E + (1-\alpha)*CE] \quad (26)$$

Here, the error and, the change in error are depicted as E and CE respectively as well as control parameter is represented with 'u'. If E value is higher one then it designates that unbalanced state of system. When the system is not in a balanced state, then FLC have to be compelled to extend the parameter 'u' until the system attains a fair position. In case of lower value of E, the system said to be closer to the balanced position.

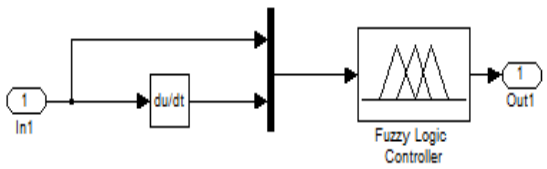

Fig.15: FLC in simulation

6. Simulation results:

The modeling of inverter control circuitry so that determination of the internal and external transfer functions was applicable in estimation of simulations which prepared for validation of the numerical representation. These are provided through MATLAB/Simulink. Table.2 shows the parameters used in the inverter performance.

Table.2: Project specifications

Variable	Project value
f_s	20 kHz
P_{out}	2 Kw
V_1	500 V
V_{C1}	250 V
V_{C2}	250 V
V_{CA}	127 V rms
V_{array}	400 V
ΔI_{Lmax}	5%
ΔV_{Cmax}	2.5%

FLC transfer functions obtained from simulation are responsible for the time response Plots of NPC control loops as shown in Fig.16. These responses are graphical representation of current flows into the grid and voltage across capacitive bus. Fig 17 and 18 are provided for the PV output voltage and active power of load here.

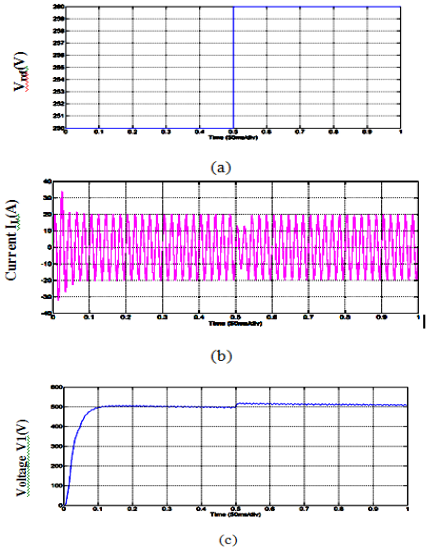

Fig.16: controllers performance on (b) the injection of current into the grid (red) and (c) the capacitive bus voltage of inverter(blue) by means of reference voltage having a perturbation of 10V in the capacitive bus.

Fig.17: PV output voltage

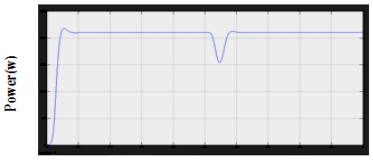

Fig.18: Load active power

6.1. THD analysis:

THD is the addition of voltage or current harmonic components of a particular voltage or current waveform which might contrast with the fundamental component of respective waveforms. Sinusoidal PWM method is provided in this structure for providing suitable switching sequence to each multilevel inverter. The switching angles of inverter switches might estimate in the above method in order to mitigate the selective harmonics.

$$\%THD = ((I_2^2+I_3^2+I_4^2+\ldots..+I_n^2)^{1/2}) \; I_1$$

Where, I_1=Fundamental Current magnitude

I_2=magnitude of 2nd harmonic
I_3= magnitude of 3rd harmonic
I_n=magnitude of nth harmonic

The expression mentioned before was provided for THD computation in case of current harmonic component. For the existing systems, which uses conventional control strategy provides load current with THD as 29.19%, which is low efficient situation for the two stage inverter to inject current with less disturbances into the lattice. In this situation FLC is used for effective controlling of converter current with THD as 4.40%, which is efficient for load current injection for providing better operating conditions. This is demonstrated in THD analysis shown in the Fig.19, and 20.

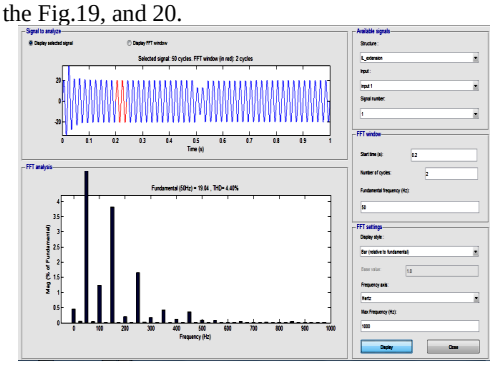

Fig.19: %THD for current wave with FLC

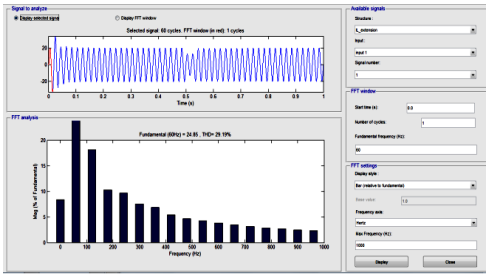

Fig.20: %THD for current wave with conventional PI controller

7. Conclusion

A two stage isolated multilevel inverter arrangement along with control methodology for converter output using FLC was proposed in this paper. DC-DC converter stage was presented for equivalent voltage distribution on inverter bus through soft switching and higher switching frequencies. NPC multilevel inverter stage provided for injecting controlled current through the utility grid. The controlling of converter parameters was processed by using FLC in the inner and outer control loops which provided for infusing electricity into the grid with less disturbance i.e., with lower THD in the current for better operation. The information available from the simulation of the structure might tested the performance of the control mechanism, through which it proved that outlets provided for such applications that are efficient and reliable in each situation of operation.

Acknowledgement

I am grateful to my guide K. Jithendra Gowd, M.Tech., Ph.D. Assistant Professor, Department Of Electrical Engineering, for his indispensable encouragement to complete the project.

References

[1] Remei Haura Junior; Marcio Mendes Casaro, "Single-Phase Dual-Stage Isolated Multilevel Inverter Applied to Solar Energy Processing", IEEE transactions on solar energy, 11th July, 2017.
[2] Y. Kim, H. Cha, B.-M. Song, and K. Y. Lee, "Design and control of a grid-connected three-phase 3-level NPC inverter for BIPV systems," in 2012 IEEE PES Innovative Smart Grid Technologies (ISGT), 2012, pp. 1–7.
[3] Agência Nacional de Energia Elétrica (Brazil), "Map book de energia elétrica do Brasil." 2008. [4] D. Watts and R. Ariztía, "The power emergencies of California, Brazil and Chile: lessons to the Chilean market," in Power Engineering 2002 Large Engineering Systems Gathering on, LESCOPE 02, 2002, pp. 7– 12.
[5] Frankfurt School, "Worldwide Trends in Renewable Vitality Investment 2015," 2015. [Online]. Accessible: http://fsunep- centre.org/productions/worldwide patterns sustainable energy investment- 2015. [Accessed: 20-Jan-2016].
[6] F. C. Mattos, V. S. Lacerda, R. L. Valle, A. A. Ferreira, P. G. Barbosa, and H. A. C. Braga, "Commitment To The Study Of A Single-Phase And Single Stage Photovoltaic Framework," IEEE Lat. Am. Trans., vol. 13, no. 5, pp. 1265– 1271, May 2015.
[7] K. C. A. de Souza, R. F. Coelho, and D. C. Martins, "Proposta de um Sistema Fotovoltaico de Dois Estágios Conectado à Rede Elétrica Comercial," Rev. Eletrônica Potência, vol. 12, no. 2, pp. 129– 136, 2007.
[8] M. Mao, Y. Zheng, L. Chang, and H. Xu, "A singlestage high increase current source inverter for network associated photovoltaic framework," in Power Electronics and ECCE Asia (ICPE-ECCE Asia), 2015 ninth International Conference on, 2015, pp.1902–1907.